Characterization of Karst Features in the Mishrif Formation (Zubair Field): Integrating Petrographic, Stratigraphic, and Tectonic Analysis for Reservoir Quality Assessment

Muhaimen Mutar Al-Janaby[(1)*], Fahad M. Al-Najm[(1)], Ali Z.Almayahi[(1)]

[1] Department of Geology, College of Science, University of Basrah, Basra, Iraq

abstract

The Mishrif Formation in the Zubair Oil Field of south Iraq is a very complex carbonate ramp reservoir of mid-Cretaceous (Cenomanian–Early Turonian) age. In addition to primary depositional conditions, meteoric karstification resulting from subaerial exposure events has the greatest control on reservoir quality. This study combines thin-section petrography, facies determinism, sequence stratigraphy and tectonic controls to describe the genesis of secondary karstic porosity and its effects on reservoir quality. Secondary pore types were identified and classified by vacuum-impregnation with blue-dyed epoxy for samples taken from a key well suite (ZB-40, ZB-43, ZB-47, ZB-49, ZB-114, ZB-195 and ZB-199).

Results indicate that meteoric karstification is facies selective and very deterministic. The high energy and grain-supported and framework-supported facies (shoal grainstones, rudist rudstones and boundstones) were highly unstable aragonitic bioclasts (rudists and bivalves) that served as extremely "reactive" "reactor beds. These facies experienced a high degree of dissolution, resulting in many coalescent vugs, "megamolds" and channel networks (karst "super-highways" with porosity in excess of 25-35% and permeabilities in excess of 100 to 1000 mD). Mixed grain-matrix packstones are moderately karstified (porosity is 14-25%, and permeability is 1-50 mD), and are characterized by moderate, but patchy, karst enhancement with the tectonic fractures serving as "super-connectors" between isolated moldic pores. Mud-supported mudstones and wackestones are low permeability aquitards and baffles (porosity < 5%, permeability < 0.1 mD), dissolution only occurs on tight local fracture pathways.

Major 3rd order sequence boundaries are periods of extended subaerial exposure, which lead to deep and significant karst overprints; maximum flooding surfaces are intra-reservoir seals. The four anticlinal domes (Hammar, Shuaiba, Rafdhia, and Safwan) developed during the depositional period creating bathymetric paleo-highs that led to rudist shoal deposition and prolonged subaerial exposure. The extensive fracture networks formed by tectonic compression were essential to the vertical plumbing system needed to get the aggressive meteoric fluids into the formation. This integrated multi scale model is a powerful predictive model to map reservoir quality and identify "sweet" spots and drilling hazards in uncored portions of the Zubair Field.

Keywords: Mishrif Formation, Zubair Oil Field, Karstification, Facies Determinism, Sequence Stratigraphy, Secondary Porosity, Reservoir Quality, Carbonate Petrography.

1. Introduction

1.1 Background and Significance

The Mishrif Formation of the mid-Cretaceous is a significant carbonate successions that were deposited on a homoclinal carbonate ramp in the Arabian Plate, including the Zubair Oil Field, southern Iraq [1]. The succession is made up of a variety of carbonate facies, from mudstone through to wackestone, packstone, grainstone, rudstone and boundstone [2]. These facies are thought to have formed in a variety of restricted lagoon to high-energy shoal, rudist bank and open marine environments [1, 2].

The reservoir quality, particularly from the upper Mishrif is strongly overprinted and influenced by meteoric karstification during subaerial exposure events [3] while depositional conditions set the basic fabric of the rocks. In the context of karstification, these complex secondary pore systems—such as vugs, dissolution channels, fissures and localized cavernous zones—play a fundamental role in the reservoir storage capacity, flow behavior and drilling characteristics [3, 4].

The main idea underlying this research is that the development of the secondary karstic porosity is not random but it is a highly determinate predictable process, under the control of a “facies-selective diagenesis” (facies determinism). The initial petrophysical properties (porosity and permeability) of the rocks, as well as the susceptibility of different rock fabrics to meteoric dissolution, were controlled by the primary depositional environment [3, 5]. The highly permeable, grain supported and rudist-rich facies contained metastable aragonitic bioclasts (rudists, bivalves) that served as highly reactive conduits for aggressive meteoric fluids. Mud-supported facies (mudstones and wackestones) provided high barriers to fluid flow (low permeabilities) and only dissolution occurred in structurally-controlled pathways [5, 6].

Two overarching regional controls superimpose this depositional template: (1) the sequence stratigraphic template that controlled the timing, duration, and lateral extent of subaerial exposure and (2) the active tectonic template that controlled the structural architecture (anticlines, faults and fractures) that guided meteoric fluid flow and served as the primary plumbing system of the karst network [7].

The study of the complexity of this reservoir needs a thorough reconstruction of the diagenetic environments and fluids that migrated through these carbonate rocks. Petrographic analyses of core thin sections are extremely important for the characterization of the interaction between early stages of marine phreatic, meteoric vadose and deep burial diagenesis [8]. Under polarized light, the chemical and isotopic composition of old fluids had a massive role in dissolving unstable minerals and the analysis of these rock fabrics offers important clues to the evolution of the pore network into its present form [9].
In addition, the reservoir properties in Mishrif Formation are different in various structural domes of Zubair Oil Field. Thickness and distribution of high energy shoal facies were directly affected by the syndepositional growth of certain domes, e.g., the Rafidiya and the Safwan domes [10]. Detailed core-plug petrophysical measurements, coupled with petrographic analysis, throughout these structural zones can enable a better characterization of rock properties and fluid-conduction capacities [11].
Finally, it is important to understand the distribution and intensity of these pathways related to karst for contemporary reservoir engineering and modelling. When operating in highly karstified zones, operations may be severely compromised during drilling by the occurrence of large mud losses, but when managed properly, this type of zone can also be the most productive [12]. Therefore, the development of an accurate predictive model for integrating Facies determinism, Sequence stratigraphy and tectonic fractures is essential to optimise the well positioning, target higher permeability formations and minimise geohazards during the field development [13].

1.2 Study Area

The research will be based on the Zubair Oil Field which is located in the tectonically active Mesopotamian foreland basin, of southern Iraq. There has been progressive structural development since the Pre-Jurassic period with the movement of the Hormuz salt, the reactivation of deep seated basement faults and the continuing collision between the Arabian and Eurasian plates.
The Zubair Field is structurally divided into four large progressive anticlinal domes, namely:
1. Hammar
2. Shuaiba
3. Rafdhia (Rafidiya)
4. Safwan

These anticlinal structures developed during the Late Cretaceous, as a continuous paleo-high on the seafloor [14]. The structural highs directly affected sedimentation by controlling the distribution of thick, high-energy, rudist-rich shoal facies on their crests [15]. Later, when the sea-level dropped relatively, the crestal areas were most exposed to the atmosphere and least flooded, and were therefore the most severely affected by aggressive meteoric diagenesis and the most highly karstified. Also, these anticlines formed thick fracture zones, which created important vertical and lateral pathways for the deep meteoric water infiltration.
The geographic and structural distribution of the wells analysed in this study shows the location of the wells in different paleogeographic positions along this carbonate ramp during Cenomanian–Early Turonian.

1.3 Research Objectives

To understand the multi-layered relationships between depositional facies, diagenetic overprints, and structural features, this study aims to achieve the following objectives:
1. Establish a detailed depositional facies framework for the Mishrif Formation in the Zubair Field to define the primary petrophysical "templates" prior to karstification.
2. Systematically identify and classify secondary pore types and karst features at the micro-scale using high-resolution petrographic criteria.
3. Analyze the diagenetic stages and reconstruct the paragenetic sequence to place meteoric karstification within the broader burial history of the basin.
4. Evaluate the relative roles of depositional facies (facies determinism), sequence stratigraphy, and tectonic fracturing in controlling karst intensity and spatial distribution to build a predictive model for reservoir quality.

1.4 Dataset and Integrated Methodology

This study is based on an integrated multi-scale geological dataset from a representative set of wells distributed across the structural domes of the Zubair Oil Field: ZB-40, ZB-43, ZB-47, ZB-49, ZB-114, ZB-195, and ZB-199. The main technique employed is that of core-slab observations with detailed thin-section petrography. Open secondary porosity, pore connectivity and micro-fractures were highlighted and mapped with impregnation of the core samples with blue-dyed epoxy performed under vacuum. The systematic study of the thin sections was used to look for diagnostic karst features, which were then classified using a hierarchical system that corresponds to the extent of meteoric alteration.
The following steps are the simplified petrographic steps used to identify and profile karst features:
1. **Blue-Epoxy Scanning:** Mapping all blue-stained regions under plane-polarized light to delineate open or partially open porosity networks.
2. **Pore-Type Classification:** Categorizing identified pores based on established diagnostic criteria, distinguishing between fabric-selective (e.g., moldic) and non-fabric-selective (e.g., vuggy, channel, fracture-enhanced, and collapse-breccia) porosities.
3. **Facies Contextualization:** Integrating the petrographic karst signatures back into the depositional facies framework to differentiate between facies-controlled matrix dissolution and structurally guided fracture dissolution.

4. **Karst Intensity Profiling:** Integrating core-scale observations with thin-section micro-features to assign a qualitative karst intensity grade (Weak, Moderate, or Strong) to the studied intervals.

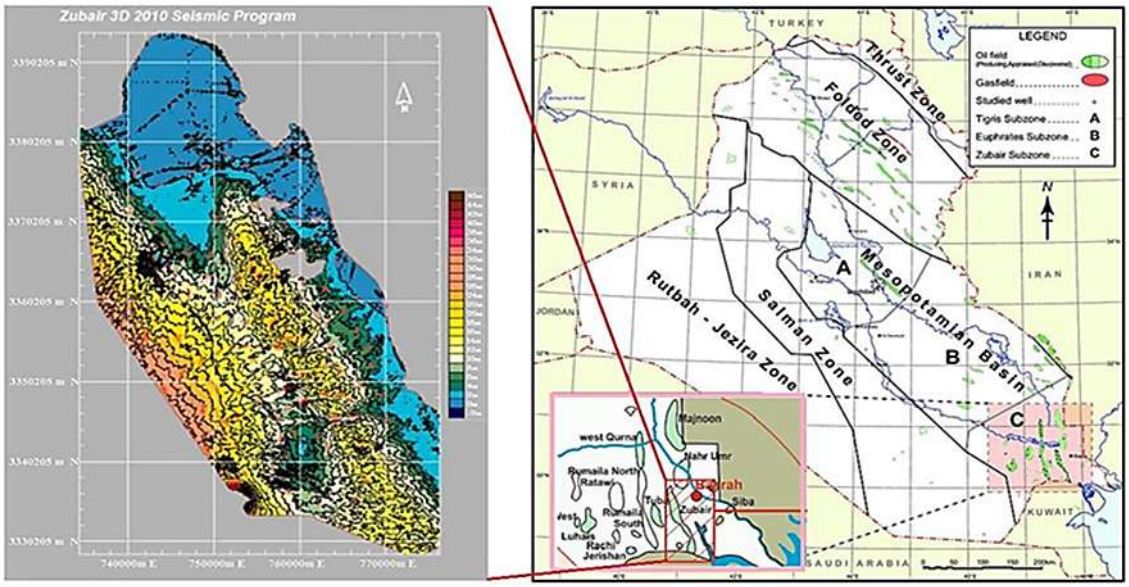

Figure 1. Regional position of the Mishrif Formation within the Zubair Oil Field study framework and the selected wells used in this study (ZB-40, ZB-43, ZB-47, ZB-49, ZB-114, ZB-199, and ZB-195).

Figuer 1 The map illustrates the structural context and the spatial distribution of wells across the field, representing different paleogeographic positions on the Cenomanian–Early Turonian carbonate ramp

2. Geological Framework

2.1 Depositional Facies and Ramp Architecture

The mid-Cretaceous Mishrif Formation in the Zubair Oil Field was deposited as a broadly homoclinal carbonate ramp with a predictable sequence of facies belts extending from a restricted inner ramp lagoon to an outer ramp and open marine basin [15]. The sedimentological template consists of several key facies types that governed the initial petrophysical properties and subsequent susceptibility to meteoric alteration [16]:

- **Mudstone and Wackestone Facies:** Deposited in restricted to open lagoons and low-energy inner ramp environments. These rocks are dominated by a tight, micrite-rich matrix with low skeletal grain density. The initial matrix porosity is low (less than 8%) with very low permeability, rendering these rocks highly impervious to pervasive fluid flow and causing them to act as background aquitards
- **Packstone Facies:** Formed under moderate-energy conditions in back-shoal and shoal-margin environments [17]. This facies is characterized by a mixed grain-matrix fabric containing skeletal grains and peloids in a partially mud-supported matrix. It possesses moderate primary porosity (5-15%) and moderate permeability (0.1-10 mD), with fluid flow focused in grain-rich patches [18].
- **Grainstone Facies:** Deposited in high-energy shoal crest environments. These rocks are well-sorted, grain-supported, and exhibit high primary interparticle porosity (15-30%) and permeability (10-1000+ mD) [19, 20]. Due to the lack of micritic matrix and an abundance of metastable aragonitic bioclasts, these are the most chemically reactive rocks in the succession.
- **Rudstone and Boundstone Facies:** Representing rudist banks, bioherms, and proximal platform margin facies [21]. These units provided the primary conduits for meteoric fluid entry during subaerial exposure, demonstrating a strong genetic relationship between high-energy deposition, diagenetic overprint, and reservoir enhancement [22].

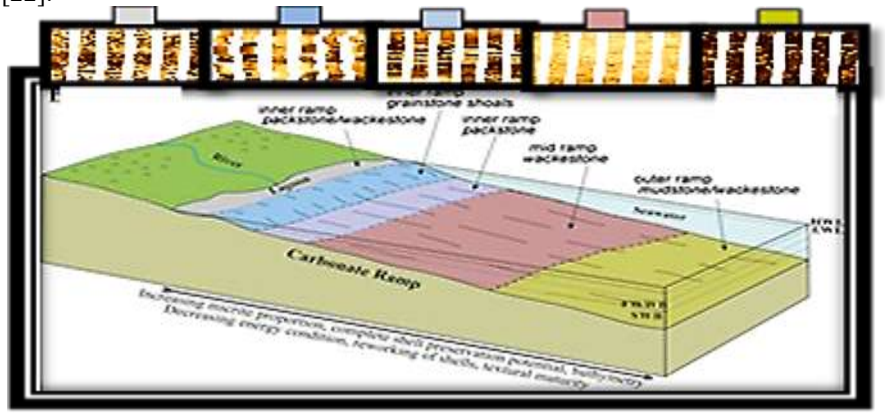

Figure 2. Conceptual model illustrating the deterministic control of depositional facies on the style and intensity of karstification in the Mishrif Formation.

Three-dimensional block diagram of the homoclinal carbonate ramp depicting depositional environments from inner ramp lagoons to high-energy shoal crests, rudist banks, and open marine environments.

2.2 Sequence Stratigraphic Control on Exposure

The sequence stratigraphic framework of the Mishrif Formation (Cenomanian–Early Turonian) is part of the Wasia Group, representing the upper part of the Arabian Plate mega-sequence AP8 [23]. The stratigraphic architecture consists of two major third-order regression cycles, within which five parasequences of transgressive-regressive (T-R) cycles are recognized.

Within this framework, regional maximum flooding surfaces (MFS)—specifically K-135 in the lowermost part and K-140 in the middle part—represent periods of maximum relative sea-level rise [24]. These surfaces are characterized by deeper-water, mud-supported facies that function as low-permeability vertical flow barriers and segment the reservoir.

In contrast, third-order sequence boundaries are marked by prolonged subaerial exposure events associated with relative sea-level falls [25]. The duration of these exposure events directly controlled the intensity of meteoric dissolution:

- **Major Sequence Boundaries (Third-Order):** Characterized by prolonged exposure, resulting in deep, intense karstification [26].
- **Parasequence Boundaries (Fourth-Order):** Characterized by shorter-lived exposure, resulting in localized and subtle dissolution features [27].

The progradation of highstand rudist lithosomes immediately beneath these sequence boundaries placed highly reactive, aragonitic, grain-supported facies in direct contact with descending meteoric waters, making these zones prime targets for high-quality karst reservoirs [28].

2.3 Tectonic Context and Anticlinal Growth

The Zubair Oil Field is located within the Mesopotamian foreland basin along the unstable continental shelf zone of the northern Arabian Plate [29]. The structural grain of the field is defined by four distinct anticlinal domes: Hammar, Shuaiba, Rafdhia, and Safwan [30]. Folding has been active from the Pre-Jurassic to the present, driven by a combination of Hormuz salt halokinesis, basement fault reactivation, and regional plate collision.

This tectonic development exerted two major controls on karst development:

1. **Sedimentary Control:** Syndepositional anticlinal growth resulted in structural paleo-highs during the Cenomanian. These bathymetric highs guided the deposition of thick, high-energy, rudist-dominated shoal facies directly on the crests of the growing anticlines [12].
2. **Exposure Control:** Episodic tectonic uplift extended the duration and increased the frequency of subaerial exposure at the anticlinal crests. These crests were the first areas to emerge above sea level and the last to be submerged, thereby experiencing the longest periods of meteoric water alteration.

Furthermore, tectonic compression generated extensive fracture networks across the anticlinal crests and flanks, which acted as vertical and horizontal conduits—the "plumbing system"—guiding aggressive meteoric fluids deep into the carbonate ramp.

3. Karst Classification and Reservoir Properties

3.1 Petrographic Classification of Karstic Porosity

Thin-section petrography utilizing blue-dyed epoxy impregnation provides direct evidence of secondary porosity and allows the identification of six distinct, hierarchical micro-scale karst features reflecting increasing meteoric alteration:

1. **Blue-Dyed Epoxy Signature:** The primary indicator of open, interconnected pore space at the time of sample preparation [8]. A vivid, deep blue represents large, well-connected voids, whereas a faint blue hue indicates micro-porosity.
2. **Moldic Porosity (Fabric-Selective):** Pore spaces that preserve the external morphology of dissolved allochems (e.g., bivalves, rudists, and benthic foraminifera). This is a diagnostic fingerprint of mineralogically controlled dissolution of unstable aragonitic grains [8, 14].
3. **Vuggy Porosity (Non-Fabric-Selective):** Irregular, equidimensional to slightly elongate voids larger than individual grains (greater than 1-2 mm) that cross-cut the primary depositional fabric, showing jagged and corroded boundaries.
4. **Channel Porosity (Fabric-Guided):** Elongate, tubular, or interconnected pore networks that follow preferential flow paths, such as bedding planes, laminae, or microfractures.
5. **Fracture-Enhanced Porosity (Structurally Guided):** Linear, planar features (tectonic or diagenetic fractures) whose walls have been variably enlarged and corroded by meteoric dissolution.
6. **Brecciation and Collapse Textures (Advanced Karst):** Chaotic fabrics formed by the mechanical collapse of the host rock due to subsurface void creation and the removal of supporting matrix [8, 14].

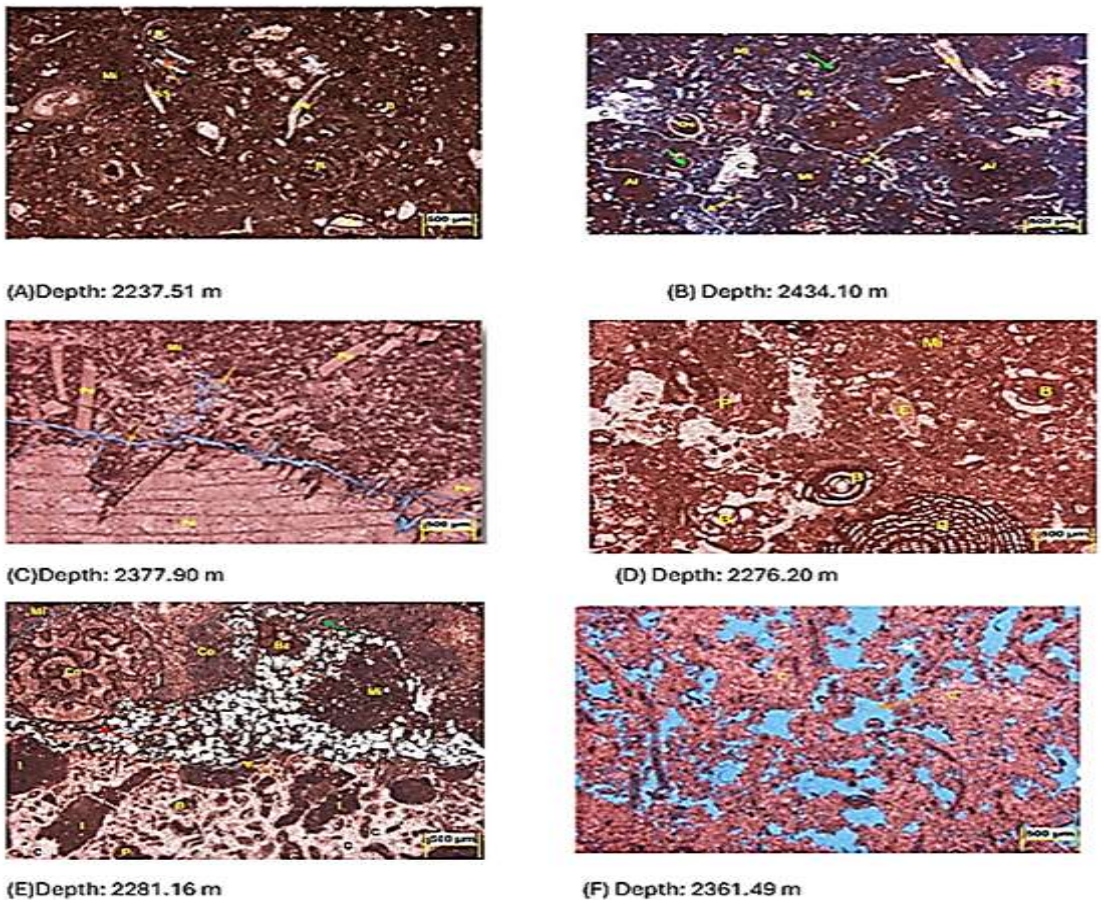

Figure 3. Petrographic criteria for recognizing karstification in Mishrif Formation thin sections.

Table 1. Summary of main karst features and their petrographic diagnostic criteria.

Karst Feature	Petrographic Expression	Likely Origin	Reservoir Significance
Moldic Porosity	Pores resembling the grain shapes (rudists, bivalves, foraminifera)	Selective meteoric dissolution of unstable allochems	Increases storage; connectivity depends on pore density and linkage
Vuggy Porosity	Unusual void spaces that are greater than single grains, filled with blue epoxy	Coalescent dissolution of adjacent molds and matrix	Good storage; moderate to high contribution to flow where interconnected
Channel Porosity	Tubular, elongated pores or interconnected pores crossing the fabric; increased fissures partially or entirely filled with blue epoxy	Dissolution focused along preferred flow paths (bedding, laminae, microfractures)	Strongly enhances connectivity and permeability; potential flow conduits
Fracture-Enhanced Porosity	Widened fractures partly or completely filled with blue epoxy	Mechanical fracturing followed by dissolution enlargement	Creates high permeability pathways; may connect otherwise isolated pores
Collapse / Cavity Porosity	Larger, irregular spaces, disturbed fabric, and brecciated structures around	Advanced dissolution and local roof collapse within karst zones	Local porosity and permeability; strong heterogeneity

3.2 Petrographic Database and Micro-scale Observations

Thin-section analyses across key reservoir intervals in the Zubair Field systematically document these micro-scale expressions of meteoric karstification.

To prevent structural redundancy, the detailed petrographic micro-photographic plates representing the distinct styles of karstification are fully integrated into their respective sessional analyses:

- The tight matrix, microvugs, and stylolite-associated dissolution characteristics of mud-supported facies are presented in **Figure 4**.
- The moldic, vuggy, and fracture-enhanced dual-permeability pore networks of the packstones are presented in **Figure 5.**
- The extreme coalescent vugs, large channels, and collapse breccias of the high-energy grainstones, rudstones, and boundstones are presented in **Figure 6**.

4. Karstification Across Carbonate Facies

4.1 Karstification in Mud-Supported Facies (Mudstone and Wackestone): The Impermeable Matrix

The mudstone and wackestone facies were deposited in restricted to open lagoonal and low-energy inner ramp environments [11]. They are characterized by a fine, micrite-dominated matrix with very low initial porosity (less than 8%) and permeability [11]. Consequently, these facies do not host extensive karst systems but act as critical low-permeability aquitards that compartmentalize the reservoir [11].

For any dissolution to occur, undersaturated meteoric waters must first breach these tight rocks [11]. The most frequently used conduits are [11]:

- Microfractures and small fracture networks [11, 15]
- Stylolites and pressure-solution seams [11, 15]
- Skeletal molds [11, 15]
- Thin permeable interbeds [11, 15]

Karstification in mudstones and wackestones is typically subtle and localized [11, 16]. The following features are characteristic: narrow, irregular microvugs (less than 0.5 mm), fracture-related voids, stylolite-associated dissolution, and patchy distribution [11, 16].

Well-by-Well Descriptive Integration (Mud-Supported Facies):

- **ZB-40, Depth 2242.20 m (Lagoonal Wackestone with Isolated Microvugs):** Core section shows dense, massive wackestone with no visible macroporosity. Thin Section (Plate 1) shows a dominant micrite matrix with a single, isolated blue microvug and a hairline fracture partially filled with blue epoxy. Interpretation: Dissolution is minimal, structurally mediated, and confined to the fracture pathway. Karst has negligible impact. Matrix porosity is less than 5%, permeability is less than 0.1 mD.
- **ZB-43, Depth 2353.44 m (Wackestone with Fracture-Related Porosity):** Core section shows dense wackestone with a sharp, sub-vertical hairline fracture. Thin Section (Plate 4) shows that fracture walls are irregular and corroded. The central fracture plane is filled with a thin but continuous train of blue-dyed epoxy. Interpretation: The tectonic fracture provided the only pathway for aggressive fluids. Karst locally enhanced vertical permeability by 1-2 orders of magnitude.
- **ZB-114, Depth 2268.49 m (Dolo-Wackestone with Stylolite-Associated Dissolution):** Core section shows dense, dolomitic wackestone with a high-amplitude, dark, clay-rich stylolite seam. Thin section of rock (Plate 127) reveals tightly packed microcrystalline dolomite with a continuous series of tiny, isolated, bright blue microvugs that are aligned perfectly with the stylolite seam. Interpretation: The stylolite served as a horizontal pathway for fluid movement and karst caused a small amount of horizontal storage within the strata. The matrix porosity is estimated at about 5% and permeability is considered negligible.

The subtle and localized nature of meteoric dissolution in tight, micrite-dominated fabrics is well documented across the low-permeability reservoir intervals. In these mud-supported mudstones and wackestones, the development of secondary porosity relies almost entirely on pre-existing structural conduits such as microfractures, hairline cracks, and stylolite seams rather than pervasive matrix flow. The micro-scale features of this restricted dissolution style are illustrated in Figure 4.

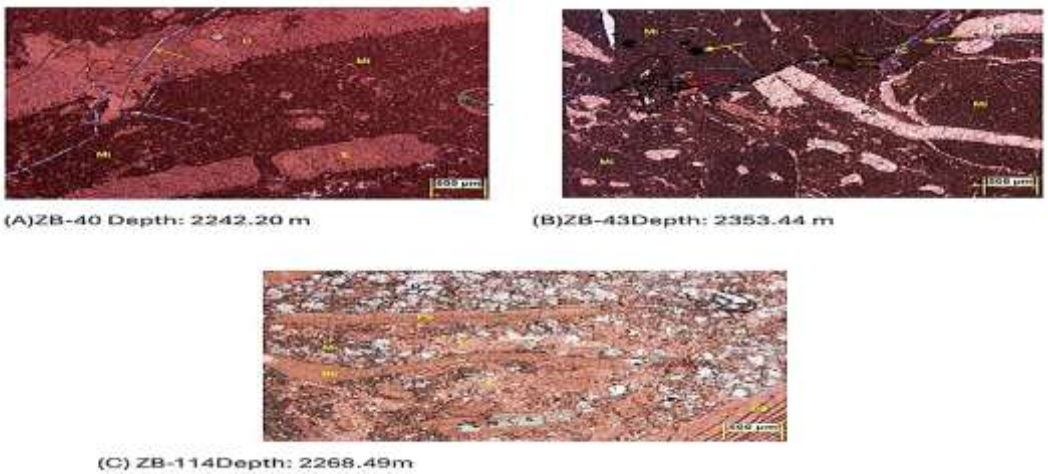

Figure 4. Karst expression in mud-supported facies.

4.2 Karstification in Packstone Facies: The Transitional Reservoir

Packstone facies represent a textural and diagenetic interface between mud-supported and grain-supported rocks. They were deposited primarily in open lagoon, back-shoal, and shoal-margin environments. Typically, packstones contain 10-50% micrite; the remainder consists of grains that are partially in contact, forming a mixed grain-matrix framework.

The importance of this mixed fabric is that it creates a dual-permeability system: grain-rich zones provide primary flow pathways, while the micritic matrix acts as a micro-scale baffle. Consequently, packstones are significantly more susceptible to meteoric modification than mud-supported facies.

On entering a packstone, undersaturated meteoric water preferentially flows through the more permeable, grain-rich zones [11, 17]. The dissolution process typically entails [11, 17]:

- Selective dissolution of unstable grains (aragonitic rudists, bivalves, and foraminifera) [11, 17]
- Expansion of interparticle space [11, 17]
- Connection of adjacent molds and vugs [11, 17]

In thin section, karstified packstones display a spectrum of features including moldic pores (abundant, well-defined cavities), irregular vugs (larger than single grains), semi-connected pore clusters (trains of blue-filled pores), and partially dissolved grains (ghost structures) [11, 18].

Table 2. Thin sections illustrating karstification in packstone facies across different wells.

Well	Depth (m)	Rock Type	Karst Features
ZB-47	2434.10 m	Algal packstone	Common moldic, secondary intragranular, fracture and intercrystalline vugs
ZB-49	2377.90 m	Pelecypods wackestone/packstone	Partially connected blue filled pores, irregular dissolution cavities
ZB-199	2237.51 m	Benthic forams packstone	Well developed moldic, intercrystalline, and fracture enhanced porosity
ZB-43	2361.49 m	Coral boundstone (packstone texture)	Vuggy and moldic porosity with good connectivity

Well-by-Well Descriptive Integration (Packstone Facies):

- **ZB-49, Depth 2377.90 m (Pelecypod Packstone with Connected Moldic-Vuggy Network):** Core section shows bioclastic packstone with scattered interparticle and moldic vugs. Thin Section (Plate 12) shows moldic pores after pelecypod shells completely dissolved, leaving thin micrite envelopes. Several adjacent molds are coalescing into larger vugs. Blue epoxy fills both pores and connecting throats. Interpretation: Karst increased porosity to 14-18% and permeability to 1-5 mD.
- **ZB-47, Depth 2434.10 m (Algal Packstone with Abundant Moldic Porosity):** Core section shows homogeneous, "sugary" texture from high density of tiny dissolution pores. Thin Section (Plate 136) shows a pervasive "Swiss-cheese" texture of densely packed, blue-filled moldic pores after aragonitic foraminifera, algae, and peloids. Interpretation: Karst transformed a moderate packstone into a high-porosity (20-25%), good-permeability (10-50 mD) reservoir rock.
- **ZB-199, Depth 2237.51 m (Benthic Foraminiferal Packstone with Mixed Porosity Network):** Core section shows foraminiferal packstone with abundant dissolution vugs up to 3 mm. Thin Section (Plate 183) shows large, blue-filled moldic pores after benthic foraminifera, linked by irregular vugs. A thin, sharp fracture filled with blue epoxy cuts across the fabric, directly connecting adjacent molds. Interpretation: Classic example of fracture acting as a "super-connector". Moldic and vuggy porosity create storage (approx. 18% total porosity) and fracture-enhanced porosity creates flow pathways (permeabilities: 20-80 mD).

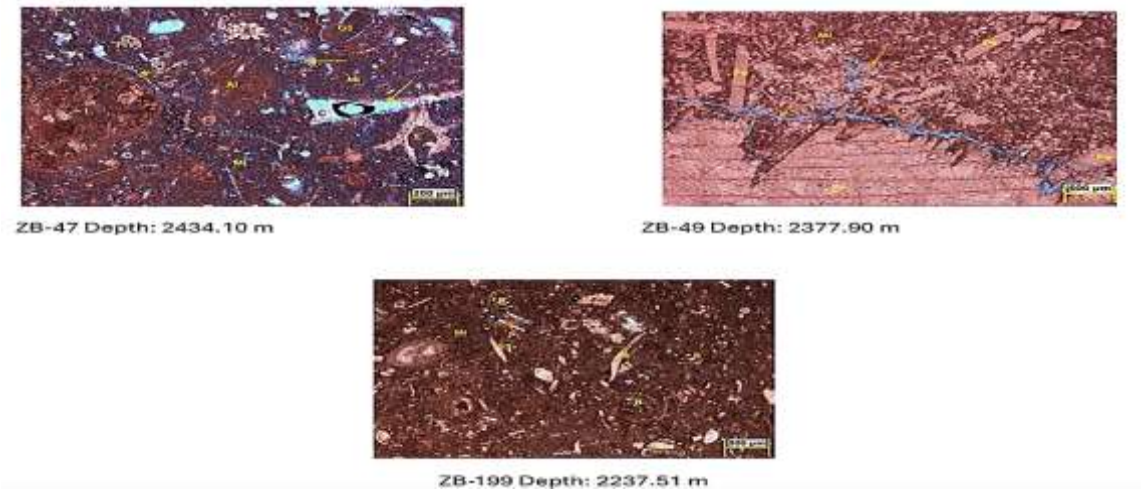

Figure 5. Karstified packstone facies

- **Description:**
  - **(A)** ZB-49, 2377.90 m (Plate 12) — selective dissolution of pelecypod shells creating moldic pores coalescing into vugs.
  - **(B)** ZB-47, 2434.10 m (Plate 136) — "Swiss-cheese" texture of densely packed, blue-filled molds.
  - **(C)** ZB-199, 2237.51 m (Plate 183) — mixed moldic, vuggy, and fracture-enhanced pore network with fracture acting as "super-connector".

4.3 Karstification in Grainstone, Rudstone, and Boundstone Facies: The Karst Super-Highways

The grainstone, rudstone, and boundstone facies represent high-energy shoal crests, rudist banks, and proximal platform-margin environments. These rocks are characterized by grain-supported or framework-supported

textures, absence of a significant micritic matrix, and abundance of large, metastable aragonitic bioclasts. They are the "reactor beds" of the Mishrif Formation, evolving into the primary karst super-highways.
When these highly permeable facies are flushed by aggressive meteoric water, they undergo a cascade of rapid dissolution processes [11, 19]:

- Unimpeded fluid flow through interparticle pores, shelter cavities, and skeletal framework [11, 19]
- Efficient dissolution of aragonitic grains, leaving large moldic pores [11, 19]
- Coalescence of pores to form large vugs and channels [11, 19]
- Fracture enlargement and linkage [11, 19]
- Collapse and brecciation in extreme cases [11, 19]

Petrographic expressions show spectacular dissolution patterns: megamolds after rudists and bivalves ("Swiss-cheese" texture), coalescent vugs (greater than 50% of thin-section view), long dissolution channels, and internal brecciation (chaotic, broken grains in blue epoxy) [11, 20].

Table 3. Thin sections showing karstification in grainstone, rudstone and boundstone facies.

Rock Type	Well	Depth (m)	Karst Features
Grainstone	ZB-49	2396.86 m	Large vugs, moldic pores, fracture enhanced porosity
Rudstone (pelecypod rich)	ZB-199	2225.71 m	Common moldic, fracture, intercrystalline and intragranular porosity
Boundstone	ZB-43	2361.49 m	Well developed vuggy and moldic pores, good connectivity
Grainstone	ZB-47	2485.33 m	Secondary inter and intragranular, intercrystalline and moldic pores

Well-by-Well Descriptive Integration (Grainstone, Rudstone, Boundstone Facies):

- **ZB-49, Depth 2396.86 m (Shoal-Crest Grainstone with Coalescent Vugs):** Core section shows clean, well-sorted grainstone with a dense network of large (up to 1 cm), interconnecting vugs. Thin Section (Plate 56) shows vast, irregular, blue-filled coalescent vugs dominating the field of view. Dissolution has consumed both grains and matrix. Interpretation: "Reservoir super-highway." Porosity 25-30%, permeability 100-1000+ mD.
- **ZB-199, Depth 2258.87 m (Pelecypod-Rich Rudstone with Channel Porosity):** Core section shows rudstone packed with large pelecypod shells. A steeply inclined, elongated, open dissolution conduit cuts through the sample. Thin Section (Plate 95) shows cross-section through a large, linear, blue-filled channel with extremely corroded walls, partly lined with carbonate mud. Interpretation: Direct evidence of focused, high-volume paleo-fluid flow. Near-infinite permeability (1000+ mD).
- **ZB-43, Depth 2361.49 m (Coral Boundstone with Cavernous/Collapse Porosity):** Core section shows coral boundstone with massively enlarged and merged primary framework cavities, creating a solution-breccia texture. Thin Section (Plate 27) shows huge, irregular, blue-filled cavities dominating the view. Remaining coral framework is partially dissolved. Local collapse occurred, creating paleo-collapse breccia. Interpretation: Ultimate karst reservoir fabric with "tank-like" storage and flow properties (porosity greater than 35%, permeability in Darcy range).

The high-energy, grain-supported and framework-supported facies—comprising grainstones, rudstones, and boundstones—represent the primary conduit system for meteoric water circulation. Lacking micritic matrix and dominated by highly reactive, unstable aragonitic bioclasts, these intervals acted as the primary "reactor beds" that focused fluid flow, resulting in extensive fabric-destructive leaching, cavernous collapse, and high-conductivity dissolution channels. The spectacular microphotographic expressions of these advanced karst networks are presented in Figure 6.

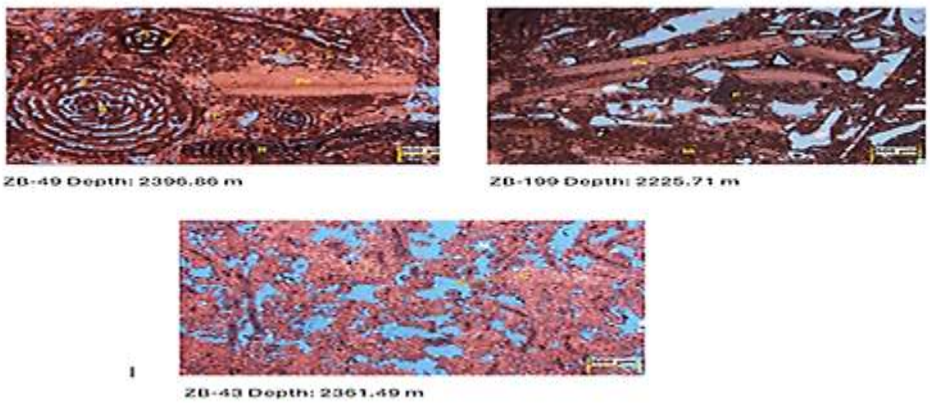

Figure 6. Karstified grainstone, rudstone, and boundstone facies — the karst super-highways.

5. Diagenetic Evolution and Alteration Environment

The karst features observed in the Mishrif Formation are the cumulative product of a multi-stage diagenetic history. This section places meteoric karstification within its full paragenetic sequence, from deposition to late burial.

5.1 Depositional Stage (Primary Fabric)

Carbonate ramp sedimentation during the Cenomanian–Early Turonian established the primary facies framework. Grain-supported facies possessed high primary porosity (15-30%), packstones had moderate (5-15%), and mud-supported facies had low (less than 5%) primary porosity.

5.2 Meteoric Diagenesis and Karstification (Subaerial Exposure)

This was the most critical stage for reservoir enhancement. Relative sea-level falls, most likely during the late Turonian–Early Coniacian, exposed the Mishrif platform top. Aggressive meteoric water invaded permeable facies and migrated along fractures and stylolites [11, 23].

5.3 Burial Diagenesis (Mesogenetic)

After burial beyond the zone of active meteoric circulation, the karstified pore system was modified by mechanical and chemical compaction (grain rotation, fracturing, crushing, and stylolitization), burial calcite cementation (blocky, drusy, or syntaxial calcite cements that selectively occluded porosity), dolomitization (ferroan dolomite rhombs replacing calcite), and late fracturing and re-opening (tectonic fractures re-connecting isolated pore clusters) [11, 22].

Table 4. Diagenetic environments, key processes, thin-section evidence, and representative examples.

Diagenetic Environment	Key Processes	Thin Section Evidence	Example from Dataset
Marine phreatic	Micritisation, isopachous cement	Micritic rims on grains; fringe cements	ZB-47, algal boundstone (Plate 12)
Meteoric vadose	Selective dissolution, meniscus cements	Irregular moldic pores, pendant cements, meniscus cements	ZB-49, pelecypod packstone (Plate 12)
Meteoric phreatic	Complete dissolution, vug formation	Large blue-filled vugs, coalescent cavities	ZB-43, coral boundstone (Plate 27)
Shallow burial	Mechanical compaction, early calcite	Broken grains, blocky calcite in pores	ZB-199, benthic forams packstone (Plate 183)
Deep burial	Stylolitisation, dolomitisation, late fractures	Stylolites with pyrite/hydrocarbons, dolomite rhombs	ZB-114, dolo-wackestone (Plate 127)

Table 5. Diagenetic stages and impact on porosity.

Stage	Main Process	Petrographic Expression	Effect on Porosity
1 – Deposition	Carbonate ramp sedimentation	Mudstone to boundstone facies framework; primary interparticle and intraparticle pores	Establishes original pore architecture; highest in grain-supported facies
2 – Early marine/near surface diagenesis	Micritization, stabilization, early marine cement	Micritized grain rims, isopachous marine cement, minor recrystallization	Slight reduction or stabilization of primary porosity
3 – Meteoric karstification	Dissolution during subaerial exposure	Molds, vugs, fissures, channels, blue epoxy filled cavities	Major creation and enlargement of secondary porosity
4 – Burial diagenesis	Mechanical compaction, stylolitization, burial cement	Grain breakage, pressure solution seams, blocky calcite cement	Reduces pore volume and connectivity in some intervals
5 – Late fracturing and re-opening	Structural fracturing and local leaching	Open or partially cemented fractures, fracture connected pores	Locally increases permeability and connects existing pore systems

6. Depositional, Stratigraphic, and Tectonic Controls on Karst Development

6.1 Sequence Stratigraphic Context and Boundaries

The Mishrif Formation in the Zubair Oil Field is composed of two major regression cycles, within which five parasequences of transgressive-regressive (T-R) cycles have been recognized. Two regional maximum flooding surfaces (MFS) have been identified: K-135 in the lowermost part of the formation, and K-140 in the middle part. These surfaces represent periods of maximum relative sea-level rise, are characterized by deeper-water, mud-supported facies, and act as low-permeability baffles that compartmentalize the karst system.

The third-order sequence boundaries identified in the Mishrif Formation are marked by karstic, exposure, and drowning features. During relative sea-level falls, the carbonate platform top was exposed subaerially, and the duration of exposure directly influenced dissolution intensity:

- **Major Sequence Boundaries (Third-Order):** Prolonged exposure; most intense karstification.
- **Parasequence Boundaries (Fourth-Order):** Shorter-lived exposure; localized dissolution features [24].

The progradation of rudist lithosomes during highstand systems tracts is particularly significant [24]. These rudist-rich facies were preferentially susceptible to dissolution during subsequent exposure. Consequently, the zones immediately beneath major sequence boundaries are prime targets for high-quality karst reservoirs.

6.2 Tectonic Framework and Structural Controls

The Zubair Oil Field is located in the tectonically active Mesopotamian foreland basin with its progressive development since the Pre-Jurassic period, as indicated by its structural grain of four progressive anticlinal domes: Hammar, Shuaiba, Rafdhia, and Safwan [3].

As these growing anticlines developed, they formed persistent paleo-highs on the seafloor which guided the deposition of rudist shoals and fracture systems which carried deep meteoric infiltration. Tectonic movement exposed or upthrew the strata, providing conditions for karstification, while fractures generated by tectonic activity improved the seepage capacity of carbonate rocks and promoted karstification [25]. This dual role of tectonics — creating both exposure framework and permeability pathways — is critical for understanding the Mishrif karst system.

Tectonic fractures play three sequential roles in the karst system:

1. **Initiation:** They form due to regional compressive stresses, salt tectonics, and basement fault reactivation [20].
2. **Fluid Pathway:** During subaerial exposure, these open fractures act as vertical and lateral conduits, channeling aggressive meteoric water deep into the formation.
3. **Enhancement:** The fractures themselves become enlarged by dissolution, evolving from tight features to wide, high-conductivity pathways.

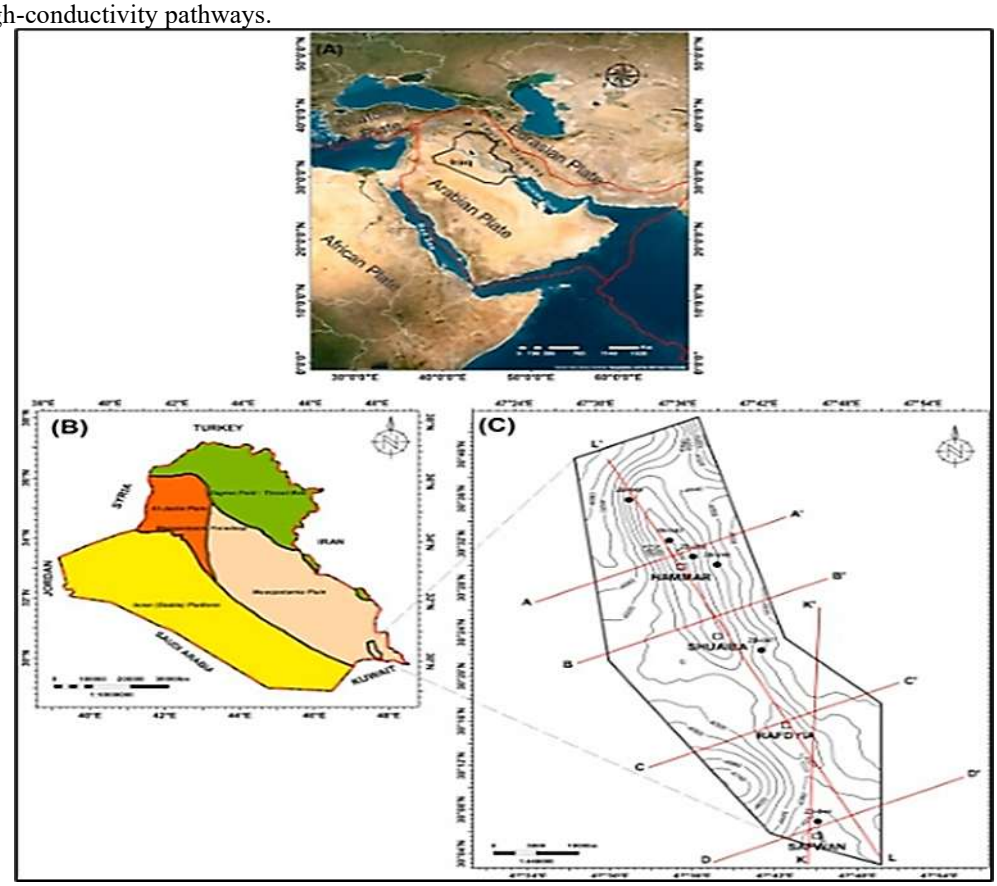

Figure 7. Tectonic framework of the Zubair Oil Field and its control on karst development.

- **Description:** (A) Regional tectonic map of southern Iraq showing the location of the Zubair Field within the Mesopotamian foreland basin. (B) Schematic structural cross-section showing the four anticlinal domes (Hammar, Shuaiba, Rafdhia, Safwan). (C) Conceptual model illustrating progressive anticlinal growth and associated fracturing creating paleo-highs for rudist shoal deposition and zones of enhanced fracture permeability that channel meteoric fluids during subaerial exposure.

6.3 Depositional Controls: The Principle of Facies Determinism

Karstification in the Mishrif Formation is facies-selective and deterministic. The depositional environment exerted a first-order control on every aspect of the subsequent meteoric overprint. The depositional facies framework dictates the initial permeability structure, which governs pathways for later aggressive fluids [11]:

- **Grain-supported facies (grainstones, rudstones, boundstones):** High primary permeability; ideal for rapid, pervasive dissolution and extensive vug/channel networks.
- **Mixed grain-matrix facies (packstones):** Moderate permeability; flow concentrated in grain-rich patches; localized and selective karstification.
- **Mud-supported facies (wackestones, mudstones):** Very low primary permeability; fluids require fractures, stylolites, or permeable interbeds; structurally mediated, low-intensity karst.

This is further enhanced by original grain mineralogy. Low-Mg calcite is far more stable than aragonite and high-Mg calcite (which are common in rudists, bivalves, corals, and some foraminifera). Hence, the highly moldic porous development is preferentially affecting the rudist-rich grainstones, rudstones, and boundstones.

Table 6. Depositional environments, dominant facies, typical karst expression, and relative impact on reservoir quality.

Depositional Environment	Dominant Facies	Typical Karst Expression	Relative Impact on Reservoir Quality
Restricted lagoon	Mudstone-wackestone	Small isolated microvugs, fracture-related pores, limited dissolution along stylolites	Low to moderate; mainly local storage, weak connectivity
Open lagoon / inner ramp	Wackestone-packstone	Dissolution of skeletal grains selectively, scattered mold and small vug	Moderate; improved storage, moderate connectivity where pore clusters develop
Back shoal / shoal margin	Packstone-grainstone	Lots of moldic and vuggy porosity with some connected (partially) pore clusters	High; good compromise between storage and connectivity
Shoal crest	Grainstone	Large vugs/cavities that have merged, tunnel-like pore networks	High to very high; potential high permeability zones with strong heterogeneity
Rudist bank / proximal platform margin	Rudstone-boundstone	Cavities and shelters for pore enlargement, irregular channels and local cavernous areas	Very high locally; excellent reservoir bodies but strongly heterogeneous

Table 7. Representative karst intervals in the studied wells: facies, petrographic evidence, and interpretation.

Well	Depth (m)	Facies (Dunham)	Karst Evidence in Thin Section	Interpretation
ZB-40	2320.5	Bioclastic Packstone–Grainstone	Blue-dyed molds after rudists and benthic foraminifera; irregular vugs partly coalescent along grain-supported layers	Karstified shoal-margin facies with moderate to good dissolution-enhanced secondary porosity
ZB-43	2308.0	Rudist-bearing Packstone	Molds after rudists and bivalves; scattered blue-filled vugs, some pores aligned along microfractures	Karst overprint on rudist-rich facies; enhanced storage with moderate connectivity and heterogeneity
ZB-47	2298.3	Grainstone	Large blue-filled vugs and coalescent cavities; elongated dissolution pores cutting the grain framework	High-energy shoal facies with strong karst dissolution; good storage and flow capacity
ZB-49	2287.6	Wackestone–Packstone	Selective dissolution of skeletal grains; microvugs and small fracture-related pores highlighted by blue epoxy	Inner-ramp facies with subtle karst modification; limited but locally important secondary porosity
ZB-114	2315.9	Bioclastic Packstone	Moldic and vuggy porosity; semi-connected blue-filled pore clusters between skeletal grains	Back-shoal facies with effective karst-enhanced porosity and improved connectivity
ZB-199	2305.2	Bioclastic Packstone–Grainstone	Enlarged dissolution pores; irregular blue-filled cavities; short connected pore trains	Well-developed karst overprint within shoal facies; good storage and flow potential

8. Paragenetic Sequence and Porosity Evolution

The present pore system of the Mishrif Formation is a composite of many diagenetic events [18]. Alternating porosity destruction and creation in different diagenetic environments leaves a porosity history in the reservoir:

- Carbonate ramp sedimentation set up the main pore structure at the Depositional Stage. Primary interparticle and intraparticle porosities were localized in the high energy, grain supported facies, and the mud supported lagoonal facies had very low primary porosities.
- Early Marine Stage: Micritisation and precipitation of marine isopachous cements resulted in a minor decrease and stabilisation of the primary interparticle pore space and prevented early compaction of the grain framework.

- Meteoric Karstification Stage: Many thorough chemical dissolutions were initiated during subaerial exposure. It was at this stage that the reservoir volume was most created, resulting in a large amount of secondary pore network created as molds, vugs, channels, and collapse breccias that greatly improved the reservoir volume storage capacity and permeability.
- Burial Stage: Compaction, pressure solution and cementation were added through deep burial diagenesis. Blocky, drusy or syntaxial burial calcite cements filled the secondary and primary pores selectively, resulting in less pore volume and connectivity, and grain breakage and stylolitization caused by compaction.
- Late Tectonic Stage: Mechanical fracturing was caused by late stage compression and structural deformation [13]. These fractures are late stage fractures that cross pre-existing cements and matrix and re-connect isolated pore clusters, locally leach the cement and re-enhance the permeability of the reservoir.

9. Reservoir Implications and Predictive Models

The use of sedimentology, diagenesis and structural geology gives a very good foundation for characterizing and predicting the reservoir quality of the Mishrif Formation throughout the area. The best reservoir quality in the Zubair Field occurs at the spatial overlap of 2 important geological trends in the field, depositional fairway of rudist-rich shoal facies and structural fairway of the anticlinal crests and highly fractured flanks.

- In order to develop such a predictive model it is possible to use this relationship to identify high quality reservoir zones, which are not being directly controlled by wells.
- Primary Karst Reservoirs: Primary karst reservoir bodies are the rudist-bioherm and shoal-crest facies (rudstones, boundstones and grainstones). The subaerial exposure has produced coalescent vuggy, moldic and channel porosity networks within these units that are excellent reservoir properties.
- The second targets are Secondary Karst Reservoirs: the back-shoal packstones and the shoal-margin packstones. These facies appear to have karst enhancement in moderate amounts but with a pattern of localised enhancement in areas of high grain content; flow is concentrated in these areas.
- Lagoonal wackestones and mudstones are intra-reservoir flow baffles (reservoir seals). Due to the micritic matrix, they were only dissolved in places, as fractures, and kept their low permeability..

10. Discussion on Multi-Factorial Karstification

The findings presented in this study demonstrate that karstification within the Mishrif Formation of the Zubair Field is a highly selective, multi-factorial process controlled by the interaction of depositional facies, sequence stratigraphy, and tectonic structure.

The tectonic framework represents the third critical control on the karst network. Syndepositional folding of the four anticlinal domes (Hammar, Shuaiba, Rafdhia, and Safwan) created bathymetric highs that guided the localized deposition of the highly reactive rudist shoals. These structural crests were subsequently exposed to subaerial conditions for the longest duration, maximizing meteoric alteration. Furthermore, tectonic stresses generated fracture networks that provided the vital vertical plumbing system required to conduct aggressive meteoric fluids deep into the formation, forming extensive fracture-enhanced conduits.

11. Conclusions

The petrographic and geological study of the Mishrif Formation in the Zubair Oil Field has been carried out at various scales, which culminated in some important conclusions that can be drawn about the development of the reservoir and distribution of the porosity.

Additionally, the extent and intensity of dissolution is clearly related to the sequence stratigraphic framework. The most important meteoric karstification intervals are related to regional third order sequence boundaries, which indicate a prolonged subaerial exposure. On the other hand, maximum flooding surfaces are intra-reservoir seals and barriers, which partition and isolate productive areas. These processes were also guided by the structural and tectonic evolution in a complementary manner. Acidic facies were formed by the dissolution of the growth of anticlinal domes (Hammar, Shuaiba, Rafdhia, and Safwan) on structural highs that had the longest period of subaerial exposure. In addition to the effects on spatial distribution, the compression of the tectonic regime created fracture networks that acted as main vertical conduits to the deep infiltration of meteoric water, thus favoring vertical karstification. Blue-dyed petrographic analysis proved effective for identifying karst-related pore systems and evaluating reservoir quality.

References

[1] Al-Dujaili, N. (2024). Reservoir and rock characterization for Mishrif Formation/ Zubair Field (Rafdiya and Safwan Domes) by Nuclear Magnetic Resonance and cores analysis. *Iraqi Journal of Chemical and Petroleum Engineering*, *25*(3), 1–14. https://doi.org/10.31699/ijcpe.2024.3.1

[2] Benthic foraminifera from Miocene sediments of the Agbada Formation, Niger Delta: Biozonation and paleoenvironmental implications. (2022). *Science Focus Journal*. https://doi.org/10.36293/sfj.2022.0081

[3] Almalikee, H. S., Almayyahi, H. K., & Al-Jafar, M. K. (2020). Karst feature in Mishrif Reservoir and effect on drilling and production in Zubair Oil Field, Southern Iraq. *Journal of Petroleum Research and Studies*, *10*(4), 19–32. https://doi.org/10.52716/jprs.v10i4.365

[4] Boschetti, T., Awadh, S. M., Al-Mimar, H. S., Iacumin, P., Toscani, L., Selmo, E., & Yaseen, Z. M. (2020). Chemical and isotope composition of the oilfield brines from Mishrif Formation (Southern Iraq): Diagenesis and geothermometry. *Marine and Petroleum Geology*, *122*, 104637.

https://doi.org/10.1016/j.marpetgeo.2020.104637
[5] Chen, P., Guo, L., Li, C., & Tong, Y. (2021). Karstification characteristics of the Cenomanian-Turonian Mishrif Formation in the Missan Oil Fields, Southeastern Iraq, and their effects on reservoirs. *Frontiers of Earth Science*, *16*(2), 435–445. https://doi.org/10.1007/s11707-020-0864-7
[6] Zhong, Y., Zhou, L., Tan, X., Guo, R., Zhao, L., Li, F., Jin, Z., & Chen, Y. (2018). Characteristics of depositional environment and evolution of Upper Cretaceous Mishrif Formation, Halfaya Oil Field, Iraq based on sedimentary microfacies analysis. *Journal of African Earth Sciences*, *140*, 151–168. https://doi.org/10.1016/j.jafrearsci.2018.01.007
[7] Ismail, M. J., Ettensohn, F. R., Handhal, A. M., & Al-Abadi, A. (2021). Facies analysis of the Middle Cretaceous Mishrif Formation in Southern Iraq borehole image logs and core thin-sections as a tool. *Marine and Petroleum Geology*, *133*, 105324. https://doi.org/10.1016/j.marpetgeo.2021.105324
[8] Huan, W., Lirong, D., Xingyang, Z., Jiquan, Y., Beiwei, L., Haigang, D., Peiguang, Y., & Yifan, S. (2024). Quantitative microfacies analyses of a carbonate ramp in the Upper Cretaceous Mishrif Formation, a oilfield in Iraq, and paleogeography reconstruction of the North-Eastern Arabian Plate. *Journal of Asian Earth Sciences*, *259*, 105896. https://doi.org/10.1016/j.jseaes.2023.105896
[9] Idan, R. M., & Salih, A. L. (2023). Reservoir quality related to diagenetic development in the carbonate Mishrif Formation: A case study from the X Oilfield, Southern Iraq. *The Iraqi Geological Journal*, *56*(2C), 100–114. https://doi.org/10.46717/igj.56.2c.8ms-2023-9-14
[10] Abbas, L. (2020). Reservoir modeling of Mishrif Formation in Majnoon Oil Field, Southern Iraq. *Iraqi Geological Journal*, *53*(1B), 89–101. https://doi.org/10.46717/igj.53.1b.6rz-02/03/2020
[11] Mahdi, T. A., Aqrawi, A. A. M., Horbury, A. D., & Sherwani, G. H. (2013). Sedimentological characterization of the Mid-Cretaceous Mishrif Reservoir in Southern Mesopotamian Basin, Iraq. *GeoArabia*, *18*(1), 139–174. https://doi.org/10.2113/geoarabia1801139
[12] Almalikee, H. S., & Sen, S. (2022). Rock-mechanical properties and in situ stress state of the Upper Cenomanian Mishrif Limestone Reservoir, Zubair Oil Field, Southern Iraq. *Interpretation*, *10*(3), T521–T529. https://doi.org/10.1190/int-2021-0109.1
[13] Abdulkariem, S. A., & Alsultan, H. A. (2026). Stratigraphic analysis of Mishrif Formation in Ratawi Oilfield, Southern Iraq. *The Iraqi Geological Journal*, *59*(1A), 274–290. https://doi.org/10.46717/igj.2026.59.1a.17
[14] Abdulaziz, A. M., Abdel, M., & Najmuddin, M. Y. (2017). Well log petrophysics of the Cretaceous pay zones in Zubair Field, Basrah, South Iraq. *Open Journal of Geology*, *7*(10), 1552–1568. https://doi.org/10.4236/ojg.2017.710104
[15] Hollis, C. (2011). Diagenetic controls on reservoir properties of carbonate successions within the Albian–Turonian of the Arabian Plate. *Petroleum Geoscience*, *17*(3), 223-241. https://doi.org/10.1144/1354-079310-032
[16] Alsharhan, A. S., & Kendall, C. S. C. (1995). Facies variation, depositional setting and hydrocarbon potential of the Upper Cretaceous rocks in the United Arab Emirates. *Cretaceous Research*, *16*(4), 435-449. https://doi.org/10.1006/cres.1995.1030
[17] Konyuhov, A. I., & Maleki, B. (2006). The Persian Gulf Basin: Geological history, sedimentary formations, and petroleum potential. *Lithology and Mineral Resources*, *41*(4), 344-361. https://doi.org/10.1134/S0024490206040055
[18] Almalikee, H. S., Almayyahi, H. K., & Al-Jafar, M. K. (2020). Karst feature in Mishrif Reservoir and effect on drilling and production in Zubair oil field, Southern Iraq. *Journal of Petroleum Research and Studies*, *10*(4), 19-32. https://doi.org/10.52716/jprs.v10i4.365
[19] Zhang, L., Zhang, W., Li, Y., Song, B., Liu, D., Deng, Y., ... & Wang, Y. (2023). Sequence stratigraphy, sedimentology, and reservoir characteristics of the middle cretaceous Mishrif Formation, South Iraq. *Journal of Marine Science and Engineering*, *11*(6), 1255. https://doi.org/10.3390/jmse11061255
[20] Al-ghafour, R. A., Al-Kubaisi, M. S., & Al-Musawy, A. D. (2022). Microfacies and Diageneses Associated Mishrif Formation in X Oilfield Southeast Iraq. *The Iraqi Geological Journal*, 127-139. https://doi.org/10.46717/igj.55.2D.11ms-2022-10-27
[21] Cantrell, D. L., Shah, R. A., Ou, J., Xu, C., Phillips, C., Li, X. L., & Hu, T. M. (2020). Depositional and diagenetic controls on reservoir quality: Example from the upper Cretaceous Mishrif Formation of Iraq. *Marine and Petroleum Geology*, *118*, 104415. https://doi.org/10.1016/j.marpetgeo.2020.104415
[22] Chafeet, H. A., Raheem, M. K., & Dahham, N. A. (2020). Diagenesis processes impact on the carbonate Mishrif quality in Ratawi oilfield, southern Iraq. *Modeling Earth Systems and Environment*, *6*(4), 2609-2622. https://doi.org/10.1007/s40808-020-00853-3
[23] Idan, R. M., & Salih, A. L. (2023). Reservoir quality related to diagenetic development in the carbonate Mishrif formation: a case study from the X Oilfield, Southern Iraq. *The Iraqi Geological Journal*, 100-114. https://doi.org/10.46717/igj.56.2C.8ms-2023-9-14
[24] Handhal, A. M., Chafeet, H. A., & Dahham, N. A. (2020). Microfacies, depositional environments and diagenetic processes of the Mishrif and Yamama formations at Faiha and Sindibad oilfields, south Iraq. *Iraqi Bulletin of Geology and Mining*, *16*(2), 51-74. https://ibgm-iq.org/ibgm/index.php/ibgm/article/view/417
[25] Mahdi, T. A., Aqrawi, A. A., Horbury, A. D., & Sherwani, G. H. (2013). Sedimentological characterization of the mid-Cretaceous Mishrif reservoir in southern Mesopotamian Basin, Iraq. *GeoArabia*, *18*(1), 139-174. https://doi.org/10.2113/geoarabia1801139
[26] Al-Mimar, H. S., Awadh, S. M., Al-Yaseri, A. A., & Yaseen, Z. M. (2018). Sedimentary units-layering system and depositional model of the carbonate Mishrif reservoir in Rumaila oilfield, Southern Iraq. *Modeling Earth Systems and Environment*, *4*(4), 1449-1465. https://doi.org/10.1007/s40808-018-0510-5

[27] Jassim, S. Z., & Goff, J. C. (Eds.). (2006). *Geology of Iraq*. DOLIN, sro, distributed by Geological Society of London.

[28] Jun, W. A. N. G., Rui, G. U. O., Limin, Z. H. A. O., Wenke, L. I., Wen, Z. H. O. U., & Tianxiang, D. U. A. N. (2016). Geological features of grain bank reservoirs and the main controlling factors: A case study on Cretaceous Mishrif Formation, Halfaya Oilfield, Iraq. *Petroleum Exploration and Development*, *43*(3), 404-415. https://doi.org/10.1016/S1876-3804(16)30047-7

[29] Al-Mohammad, R. A. H., & Abdul, R. (2012). Depositional Environment and Petrophysical Properties Study of Mishrif Formation in Tuba Oilfield, Southern Iraq. *Journal of Basrah Researches Sciences*, *38*(1A), 25-50.

[30] Boschetti, T., Awadh, S. M., Al-Mimar, H. S., Iacumin, P., Toscani, L., Selmo, E., & Yaseen, Z. M. (2020). Chemical and isotope composition of the oilfield brines from Mishrif Formation (southern Iraq): Diagenesis and geothermometry. *Marine and Petroleum Geology*, *122*, 104637.https://doi.org/10.1016/j.marpetgeo.2020.104637